Diabetologia (2012) 55:509–519
DOI 10.1007/s00125-011-2364-5

ARTICLE

Kidney-targeting *Smad7* gene transfer inhibits renal TGF-β/MAD homologue (SMAD) and nuclear factor κB (NF-κB) signalling pathways, and improves diabetic nephropathy in mice

S. M. Ka · Y. C. Yeh · X. R. Huang · T. K. Chao · Y. J. Hung · C. P. Yu · T. J. Lin · C. C. Wu · H. Y. Lan · A. Chen

Received: 26 July 2011 / Accepted: 30 September 2011 / Published online: 16 November 2011

Abstract
Aims/hypothesis The TGF-β/MAD homologue (SMAD) and nuclear factor κB (NF-κB) signalling pathways have been shown to play a critical role in the development of renal fibrosis and inflammation in diabetic nephropathy. We therefore examined whether targeting these pathways by a kidney-targeting *Smad7* gene transfer has therapeutic effects on renal lesions in the *db*/*db* mouse model of type 2 diabetes.
Methods We delivered *Smad7* plasmids into the kidney of *db*/*db* mice using kidney-targeting, ultrasound-mediated, microbubble-inducible gene transfer. The histopathology, ultrastructural pathology and pathways of TGF-β/SMAD2/3-mediated fibrosis and NF-κB-dependent inflammation were evaluated.
Results In this mouse model of type 2 diabetes, *Smad7* gene therapy significantly inhibited diabetic kidney injury, compared with mice treated with empty vectors. Symptoms inhibited included: (1) proteinuria and renal function impairment; (2) renal fibrosis such as glomerular sclerosis, tubulo-interstitial collagen matrix abundance and renal inflammation, including *Inos* (also known as *Nos2*), *Il1b* and *Mcp1* (also known as *Ccl2*) upregulation, as well as macrophage infiltration; and (3) podocyte and endothelial cell injury as demonstrated by immunohistochemistry and/or electron microscopy. Further study demonstrated that the

Electronic supplementary material The online version of this article (doi:10.1007/s00125-011-2364-5) contains peer-reviewed but unedited supplementary material, which is available to authorised users.

S. M. Ka
Graduate Institute of Aerospace and Undersea Medicine, Tri-Service General Hospital, National Defense Medical Center, Taipei, Taiwan, Republic of China

Y. C. Yeh · T. J. Lin
Graduate Institute of Life Sciences, Tri-Service General Hospital, National Defense Medical Center, Taipei, Taiwan, Republic of China

C. C. Wu
Department and Graduate Institute of Pharmacology, Tri-Service General Hospital, National Defense Medical Center, Taipei, Taiwan, Republic of China

A. Chen
Graduate Institute of Medical Sciences, National Defense Medical Center, Taipei, Taiwan, Republic of China

T. K. Chao · C. P. Yu · A. Chen (✉)
Department of Pathology, Tri-Service General Hospital, National Defense Medical Center, No. 325, Sec. 2, Cheng-Gung Road, Taipei, Taiwan, Republic of China
e-mail: doc31717@ndmctsgh.edu.tw

Y. J. Hung
Division of Endocrinology and Metabolism, Department of Internal Medicine, Tri-Service General Hospital, National Defense Medical Center, Taipei, Taiwan, Republic of China

X. R. Huang · H. Y. Lan
Department of Medicine and Therapeutics and Li Ka Shing Institute of Health Sciences, Chinese University of Hong Kong, Hong Kong, China

improvement of type 2 diabetic kidney injury by overexpression of *Smad7* was associated with significantly inhibited local activation of the TGF-β/SMAD and NF-κB signalling pathways in the kidney.
Conclusions/interpretation Our results clearly demonstrate that kidney-targeting *Smad7* gene transfer may be an effective therapy for type 2 diabetic nephropathy, acting via simultaneous modulation of the TGF-β/SMAD and NF-κB signalling pathways.

Keywords *db*/*db* mice · Diabetic nephropathy · Endothelial cell · Podocyte · SMAD7 · Type 2 diabetes · Ultrasound-mediated microbubble-inducible gene transfer

Abbreviations

BUN	Blood urea nitrogen
FLAG m2	Anti-FLAG m2 monoclonal antibody
MCP	Monocyte chemoattractant protein-1
NF-κB	Nuclear factor κB
PAS	Periodic acid–Schiff's reagent
α-SMA	α-Smooth muscle actin
SMAD	MAD homologue
VEGF	Vascular endothelial growth factor
WT-1	Wilms tumour 1

Introduction

Type 2 diabetes is a leading cause of end-stage kidney disease in the world due to diabetic nephropathy [1–3], which features progressive renal fibrosis/sclerosis and inflammation as major pathogenic pathways [4–8]. Although many therapeutic approaches focusing on hyperglycaemia and high blood pressure have been used, numerous patients still suffer from progressive and severe renal injury [9].

Anti-TGF-β monoclonal antibody [8], TGF-β receptor [2] or TGF-β receptor inhibitor [10] have been shown to be of benefit in some mouse models of diabetic nephropathy as they prevent glomerulosclerosis. Besides, renal lesions in diabetic nephropathy have higher levels of TGF-β [11, 12], while increasing evidence indicates a pathogenic role of TGF-β in the glomerulosclerosis that occurs with diabetic nephropathy [13–15]. However, although neutralisation of antibodies is effective in inhibiting TGF-β, thereby preventing renal fibrosis, it may also enhance the inflammatory response [8, 16]. By blocking the activation of MAD homologue (SMAD)2/3, SMAD7 can inhibit the TGF-β/SMAD-mediated fibrosis-signalling pathway [17, 18]; at the same time, SMAD7 blocks nuclear factor κB (NF-κB) activation by enhancing inhibitor of NF-κB (IκB)α production [19, 20]. Moreover, in our previous study, overexpression of *Smad7* in the kidney inhibited the TGF-β/SMAD-mediated renal fibrosis pathway and NF-κB-driven inflammation [21]. This prompted us to evaluate the effects of the kidney-targeting route for delivery of *Smad7* on the renal lesions associated with type 2 diabetes and to dissect the responsible mechanisms. In the present study, therefore, we delivered *Smad7* plasmids into the kidney of the *db*/*db* mouse model of type 2 diabetes using a kidney-targeting, ultrasound-mediated, microbubble-inducible gene transfer [21–23] and demonstrated therapeutic effects on the renal fibrosis/sclerosis lesions and inflammation that are characteristic of diabetic nephropathy. These effects occurred via modulation of the SMAD2/3-mediated fibrosis and NF-κB-dependent pathways locally in the kidney, as well as by the reversal of ultrastructural alterations suggestive of intrinsic glomerular cell injury.

Methods

Animal model All animal experiments were performed with the approval of the Institutional Animal Care and Use Committee of The National Defense Medical Center, Taiwan, and were consistent with the NIH Guide for the Care and Use of Laboratory Animals. Male mutant C57BLKs/J *db*/*db* mice (mouse model of type 2 diabetes) and their normal littermates (*db*/*m*, wild-type) were purchased from Jackson Laboratory (Bar Harbor, ME, USA). The *db*/*db* mice were maintained on a standard laboratory diet and water before the study, with the exception of food removal for fasting blood glucose measurements. We used 12 *db*/*db* mice per group in disease and treatment groups, respectively, and 12 age-matched *db*/*m* mice as normal control. To determine the starting point of the therapeutic intervention, we demonstrated in a preliminary experiment that although our mouse model of type 2 diabetes developed hyperglycaemia and hyperglycosuria at the age of 6 to 8 weeks, urinary albumin did not start to appear until 34 weeks of age, suggesting late development of urinary albumin, compared with its earlier manifestation at 23 to 26 weeks as described elsewhere [24, 25]. We therefore began the gene transfer in *db*/*db* mice at the age of 32 weeks.

Organ-targeted, ultrasound-mediated, microbubble-inducible Smad7 gene transfer into the kidney Preparation of a mixture of doxycycline-regulated pTRE-m2*Smad7*-expressing plasmids and gene transfer into the kidney of mice using the ultrasound-mediated, microbubble-inducible gene transfer technique were done as described previously [21]. To determine the efficacy of ultrasound-mediated, microbubble-inducible gene transfer into the kidney of the mice, groups of six *db*/*db* mice were given a mixture of *Smad7* plasmids (15 μg/g) and echocardiographic contrast

microbubbles (Optison, Mallinckrodt, MO, USA) via the tail vein, followed immediately by ultrasound treatment. After ultrasound treatment, 200 μg doxycycline (Sigma, St Louis, MO, USA) was injected intraperitoneally, followed by the addition of doxycycline to the daily drinking water (200 μg/ml). The mice were killed at days 2, 7 and 14 after *Smad7* gene transfer, and their kidneys collected for examination of *Smad7* mRNA expression by real-time PCR and of SMAD7 abundance by western blot analysis and immunohistochemistry using the anti-FLAG m2 monoclonal antibody (FLAG m2) (see Electronic supplementary material [ESM] Fig. 1 and ESM Methods). Based on the data, *Smad7* gene transfer was given every 14 days to maintain a high level of *Smad7* expression within the kidney throughout the subsequent experiment. The *db*/*db* mice that received an empty vector only served as disease control (control type 2 diabetes mice). All mice were killed at week 38 on the fifth day after the last gene or empty vector transfer.

Clinical and histopathological evaluation Collection and assay of blood and urine samples were performed as described previously [21]. Urine albumin, urine creatinine, urine glucose and serum glucose were determined at the age of 6 weeks and every 2 weeks thereafter until 38 weeks, when the mice were killed. The concentration of urine albumin was examined by ELISA (Exocell, Philadelphia, PA, USA) and urine samples were individually adjusted for urine creatinine excretion (Wako Pure Chemical Industries, Osaka, Japan). Urine glucose was measured using a test strip (Siemens, Tokyo, Japan). Serum glucose was measured as described previously [26]. At 38 weeks, 10 μl serum per mouse was collected for the measurement of blood urea nitrogen (BUN) and creatinine using BUN and creatinine (the Jaffe reaction) kits (Fuji Dry-Chem Slide; Fuji Film Medical, Tokyo, Japan), respectively. Calibration with a blank run before each sample was done using an autoanalyser (5500V; Fuji Film Medical).

For histopathological examination, the tissues were fixed in 10% (vol./vol.) buffered formalin and embedded in paraffin. Sections (4 μm) were stained with haematoxylin and eosin and periodic acid–Schiff's reagent (PAS). Scoring of glomerular mesangial expansion and/or mesangial matrix increase was determined by quantitative image analysis software (Pax-it; Paxcam, Villa Park, IL, USA) as previously described [27]. Briefly, 20 glomeruli were randomly selected from each section and positive signals within the selected glomerulus were highlighted, measured and quantified as per cent positive area of the entire glomerulus.

Confocal microscopy, immunohistochemistry and detection of apoptosis For confocal microscopy, frozen sections were stained with guinea pig anti-nephrin (Acris Antibodies, Herford, Germany), rabbit anti-vascular endothelial growth factor (VEGF) (Santa Cruz, Santa Cruz, CA, USA), which is a marker of podocyte injury related to diabetic nephropathy [28–30], or rabbit phosphorylated SMAD2/3 antibodies (Santa Cruz), followed by their relative secondary antibodies, rabbit anti-guinea pig Alexa Fluor 488 (Invitrogen, Carlsbad, CA, USA) and goat anti-rabbit phycoerythrin (Jackson ImmunoResearch Laboratories, West Grove, PA, USA). Sections were imaged on a laser scanning microscope (LSM510; Carl Zeiss, Weesp, the Netherlands) (laser intensity 20%, detector gain 600, amplifier offset 1). For detection of fibrosis/sclerosis related proteins and proinflammatory proteins, see ESM Methods. For the detection of apoptosis, TUNEL was used. Formalin-fixed tissue sections were stained using a kit (ApopTag Plus Peroxidase In Situ Apoptosis Detection kit; Chemicon, Temecula, CA, USA) according to the manufacturer's instructions. For scoring of the glomerular abundance, as determined by immunohistochemistry, of SMAD7, α-smooth muscle actin (α-SMA), collagen I, III and IV, monocyte chemoattractant protein-1 (MCP-1), nephrin, VEGF and FLAG m2, Pax-it quantitative image analysis software (Paxcam) was used as described above. The numbers of phosphorylated NF-κB p65-, phosphorylated SMAD2/3-, CD3-, F4/80- or TUNEL-positive cells were counted in 20 consecutive glomeruli and expressed as cells/glomerular cross-section. Using light microscopy, we examined 20 randomly selected fields of the tubulo-interstitial compartment in the cortical area at a magnification of ×400 and expressed values as cells per field.

Real-time PCR analysis The RNA of kidney, liver and spleen was extracted as described previously [21]. Real-time PCR was performed on a sequence detection system (ABI Prism 7700; Applied Biosystems, Foster City, CA, USA). The probes and primers of mouse β-actin (Mm00725412_s1), *Col-I* (Mm00802331_m1), *Col-III* (Mm00801666_g1), *Col-IV* (Mm00802372_m1), *Ctgf* (Mm01192933_g1), *Il1b* (Mm01336189m1), *Inos* (also known as *Nos2*) (Mm00440485_m1), *Mcp1* (also known as *Ccl2*) (Mm00802372_m1), *α-Sma* (also known as *Acta2*) (Mm00725412_s1), *Smad7* (Mm00484741_m1) and *Tgfb* (Mm0441724_m1) were assay-on-demand gene expression products (Applied Biosystems). Real-time PCR reactions were performed using 10 μl cDNA, 12.5 μl TaqMan Universal PCR Master Mix (Applied Biosystems) and 1.25 μl of the specific probe/primer mixed in a total volume of 25 μl. The thermal cycler conditions were as follows: 2 min at 50°C, 10 min at 95°C, 40 cycles of denaturation (15 s at 95°C) and combined annealing/extension (1 min at 60°C). The $2^{-\Delta\Delta C_t}$ method was used

to determine relative amounts of product using β-actin as an endogenous control. The average fold change is presented graphically.

Western blot analysis The concentration of cytoplasmic proteins was examined using a BCA protein assay kit (Thermo Fisher Scientific, Waltham, MA, USA) according to the manufacturer's instructions. We ran 50 μg of each sample on a 10% (wt/vol.) SDS-PAGE gel. The gel was electroblotted on to polyvinylidene difluoride nitrocellulose membrane (Amersham, Little Chalfont, UK), incubated for 1 h in blocking buffer (Tris-buffered saline containing 5% [wt/vol.] skimmed milk) and incubated overnight at 4°C with goat anti-SMAD7 (Santa Cruz), rabbit anti-SMAD3 (Zymed, South San Francisco, CA, USA), rabbit anti-phosphorylated SMAD3 (Biosource, Camarillo, CA, USA) or goat anti-β-actin (Santa Cruz) antibodies. After washing, the membrane was incubated for 1 h at room temperature with horseradish peroxidase-conjugated rabbit anti-goat or goat anti-rabbit (Pierce, Rockford, IL, USA) antibodies. The membrane-bound antibody detected was incubated with chemiluminescent reagent plus (Perkin Elmer Life Sciences, Boston, MA, USA) and captured on x-ray film. Semi-quantitative analysis software (Bio-CAPT; ViLber, Lourmat, France) was used to evaluate the amounts of product.

ELISA TGF-β1 protein levels in renal tissue were measured using commercial ELISA kits (R&D, Minneapolis, MN, USA) according to the manufacturer's instructions. Briefly, protein samples were acidified with 1 mol/l HCl and neutralised with 1.2 mol/l NaOH/0.5 mol/l HEPES to assay the amount of TGF-β1. Absorbance was determined at 450 nm using an ELISA plate reader (Bio-Tek, Winooski, VT, USA). NF-κB p65 activation was measured in renal tissue nuclear protein extracts using Trans-AM ELISA assay kits (Active Motif, Carlsbad, CA, USA) according to the manufacturer's instructions. Nuclear proteins were extracted using a nuclear extract kit (Active Motif).

Electron microscopy Samples were fixed in a mixture of 4% (wt/vol.) paraformaldehyde and 0.5% (wt/vol.) glutaraldehyde in PBS, pH 7.4, and prepared as described previously [31]. Ultrathin sections were cut, placed on a nickel grid and then examined under an electron microscope.

Statistical analysis Values are presented as the mean±SEM. Comparisons of urinary albumin, serum sugar, urinary glucose and the efficacy of *Smad7* expression among groups were made with one-way ANOVA, with post hoc correction by Tukey's method. Comparison between two groups was performed using Student's *t* test. A value of $p<0.05$ was considered statistically significant.

Results

Urinary albumin and renal function At 34 weeks of age, control *db*/*db* mice developed a significantly higher, and thereafter continuously increasing urinary albumin/creatinine ratio than wild type (*db*/m) mice (Fig. 1a). However, their counterparts treated with *Smad7* gene transfer by a kidney-targeting, ultrasound-mediated, microbubble-inducible gene transfer technique showed a markedly decreased urinary albumin/creatinine ratio, compared with control. Compared with control, the *Smad7*-transferred *db*/*db* mice showed significantly reduced serum

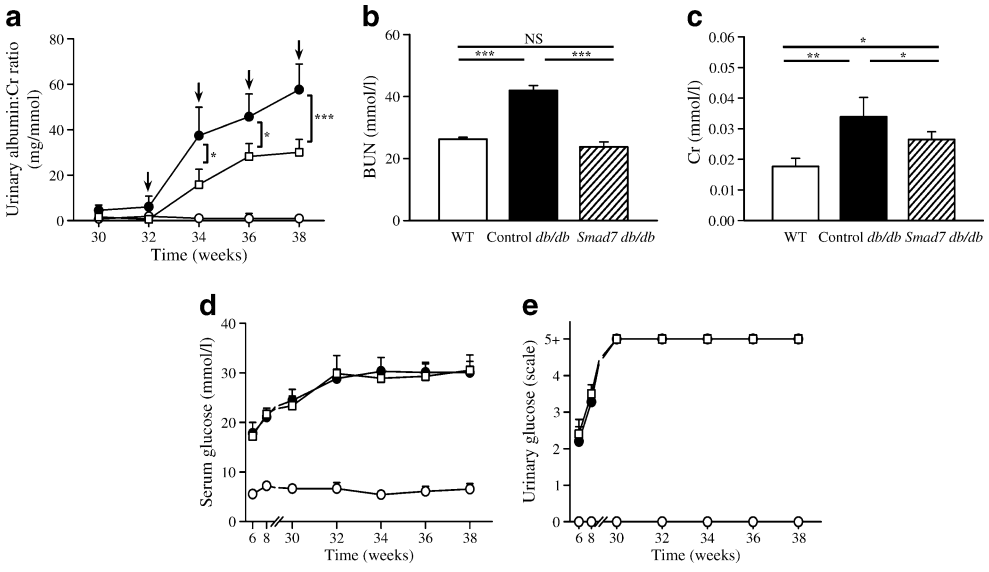

Fig. 1 Urinary albumin and renal function. **a** Time course studies of urinary albumin/creatinine (Cr) ratio. The arrows indicate the time point of *Smad7* or vector transfer. White circles, wild-type (*db/m*); black circles, control *db*/*db*; white squares, *Smad7 db*/*db*. **b** BUN, (**c**) serum creatinine, (**d**) serum glucose and (**e**) urinary glucose. Data are mean±SEM for groups of 12 mice; *$p<0.05$, **$p<0.01$ and ***$p<0.005$

levels of BUN (Fig. 1b) and creatinine (Fig. 1c) ($p<0.05$ for both), although their creatinine levels remained high compared with wild-type mice. However, both groups of *db*/*db* mice (*Smad7*, control) revealed higher levels of serum glucose (Fig. 1d) and urine glucose (Fig. 1e) than wild-type mice.

Renal histopathology and ultrastructural pathology Light microscopy revealed that control *db*/*db* mice had diffuse mesangial expansion, scattered nodular sclerosis and occasional arteriolar hyalinosis, associated with scattered mononuclear leucocyte infiltration in the interstitium (Fig. 2a–g), although the tubular compartment was largely intact compared with wild-type mice. However, these effects were substantially blunted in the *Smad7*-transferred *db/db* mice, but compared with wild-type mice, the former still revealed substantial mesangial expansion (Fig. 2c, f, g) ($p<0.05$). Mounting evidence shows that apoptosis is present in various compartments of kidney in the *db*/*db* mouse model of type 2 diabetes, including podocytes, mesangial cells, endothelial cells and tubular epithelial cells [32–35]. TUNEL analysis in renal tissues of mice showed significant suppression of apoptosis in the kidney of *Smad7*-transferred compared with control *db*/*db* mice at week 38 ($p<0.005$) (Fig. 2h–l).

Glomerular ultrastructure was examined by electron microscopy at 38 weeks when the mice were killed. Compared with wild-type mice (Fig. 2m), we observed the following in control *db*/*db* mice: (1) focal, but intense villous transformation of the podocytes associated with intervening networks in the urinary space; (2) increased cytoplasmic vesicles; (3) scattered laminar bodies and focal fusion of foot processes; (4) thickening of the glomerular basement membrane; (5) enhanced mesangial matrix deposition; and (6) fibrillar aggregates or filamentous substance in the mesangium and podocytes (Fig. 2n). In addition, endothelial cells of the diseased mice had markedly increased swelling in vesicles and cytoplasmic processes. However, the *Smad7*-transferred *db*/*db* mice showed much fewer abnormal changes in podocytes or

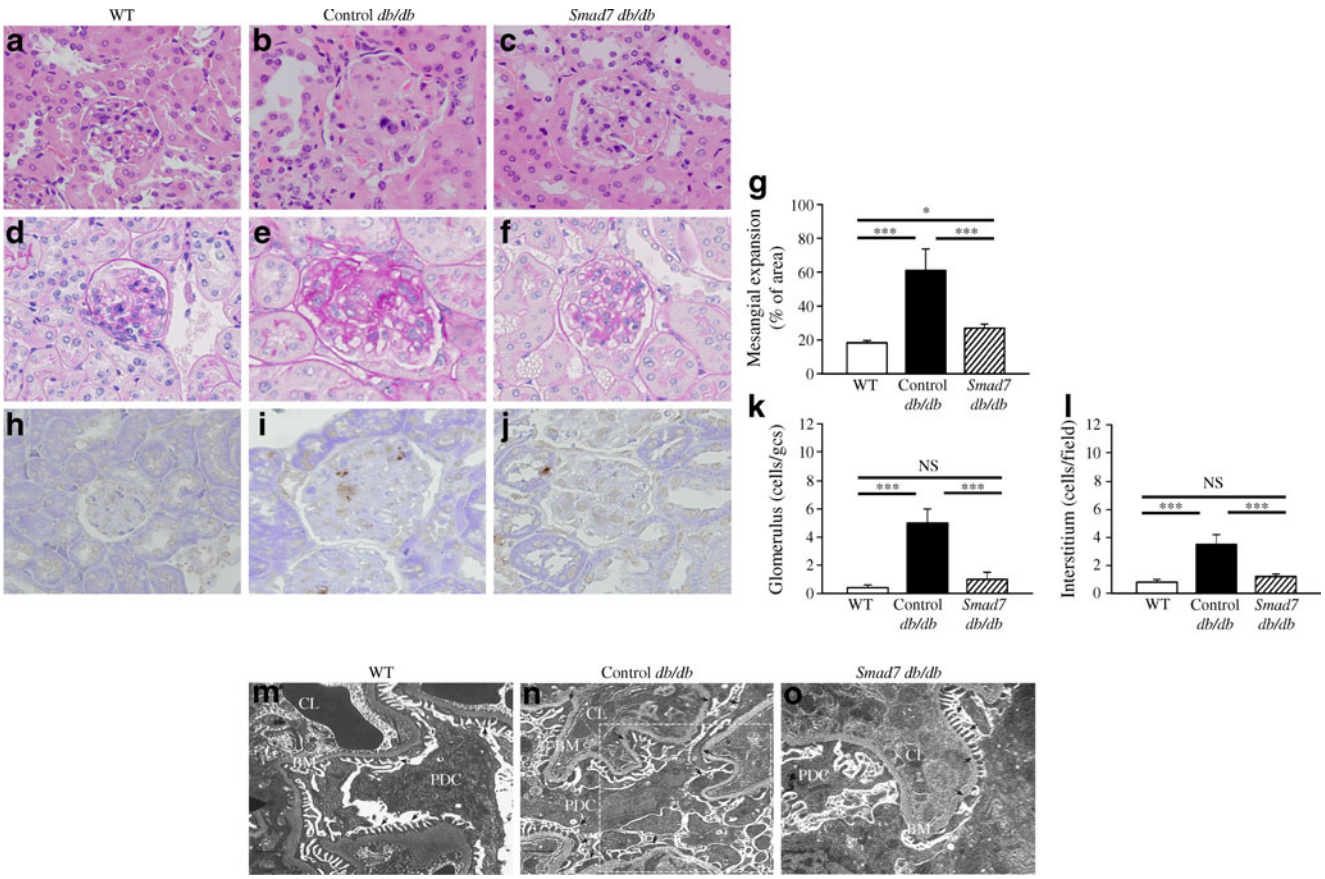

Fig. 2 Renal histopathology and ultrastructural alterations. **a–c** Haematoxylin and eosin stain of tissue as labelled. **d–f** PAS stain and (**h–j**) TUNEL stain of tissue as indicated. Original magnification (**a–f, h–j**) ×400. **g** Scoring of mesangial expansion (PAS) and (**k**, **l**) of positive cells in kidney. Values (**g**, **k**, **l**) are the mean±SEM for a group of 12 mice; *$p<0.05$ and ***$p<0.005$. gcs, glomerular cross-section. **m** Electron microscopy of wild-type (WT, *db/m*), (**n**) control *db/db* mice and (**o**) *Smad7*-transferred *db/db* mice showed (in white dashed frame) (**n**) podocytes (PDC) with villous transformation. Scale bars 2 μm, original magnification electron microscopy ×6,000. Arrows, foot processes; CL, capillary lumen; BM, glomerular basement membrane

endothelial cells, although thickening of the glomerular basement membrane was present (Fig. 2o).

Abundance of nephrin and VEGF in podocytes The effects of *Smad7* gene transfer on podocytes was further evaluated by confocal laser scanning microscopy to determine the correlation of nephrin (a podocytes marker) and VEGF abundance in the kidney, because these proteins have major implications for the pathogenesis of diabetic nephropathy. As shown in Fig. 3, although control *db*/*db* mice revealed significantly enhanced glomerular VEGF abundance in podocytes (19.7±10.5%) compared with wild-type mice (3.2±1.8%) ($p<0.01$), their *Smad7*-transferred counterparts showed only faint staining of the protein in podocytes (5.6±0.2%) compared with control ($p<0.01$). In contrast, the latter group (*Smad7*-treated) showed a significant increase of nephrin protein in the glomerulus (32.8±1.5%) compared with control mice (22.7±0.2%) ($p<0.05$), although control *db*/*db* animals had less nephrin protein in the glomeruli than wild-type mice (39.9±1.4%) ($p<0.05$).

Renal fibrosis/sclerosis-related gene expression and protein abundance Renal fibrosis/sclerosis-related gene expression was detected to determine the mechanisms responsible for *Smad7* gene therapy in this mouse model of type 2 diabetes. As shown in Fig. 4a, *Smad7* gene transfer resulted in significantly enhanced *Smad7* mRNA expression in the kidney, as detected by real-time PCR, compared with wild-type or control *db*/*db* mice ($p<0.01$ for both), confirming the *Smad7*-derived favourable effects on renal lesions in treated *db*/*db* mice. There was no significant difference in *Smad7* mRNA in liver and spleen among *Smad7*-transferred and control *db*/*db* mice, or in wild-type mice (liver: wild-type 1.1±0.5-fold change, control *db*/*db* 1.2±0.4-fold change, *Smad7*-transferred *db*/*db* 1.2±0.2-fold changes; spleen: wild-type 1.0±0.2-fold change, control *db*/*db* 0.7±0.3-fold change, *Smad7*-transferred *db*/*db* 0.8±0.3-fold change), suggesting that one advantage of this kidney-targeting gene delivery method could be the fewer potential side effects in important organs such as the liver and the spleen. Although the expression of several fibrogenic markers in the kidney was upregulated in the control *db*/*db* mice, including *Ctgf* (Fig. 4b), *α-Sma* (Fig. 4c), *Col-I* (Fig. 4d), *Col-III* (Fig. 4e) and *Col-IV* (Fig. 4f), *Smad7* gene transfer induced a dramatic suppression of these genes in the kidney of their *Smad7*-transferred counterparts ($p<0.05$ for each). The *Smad7*-transferred mice showed significantly enhanced SMAD7 levels diffusely in glomerular cells and tubular epithelial cells, compared with control *db*/*db* mice (Fig. 4g, h, ESM Fig. 2a). A striking accumulation of α-SMA (Fig. 4i, ESM Fig. 2b), and collagen I (Fig. 4j, k, ESM Fig. 2c), III (Fig. 4l, m, ESM Fig. 2d) and IV (Fig. 4n, o, ESM Fig. 2e) in the kidney of control *db*/*db* mice was demonstrated by immunohistochemistry, whereas renal SMAD7 levels remained lower (Fig. 4g, h, ESM Fig. 2a). Again, these effects were greatly inhibited by the kidney-targeting *Smad7* gene therapy in *Smad7*-transferred mice, which had moderate renal SMAD7 levels.

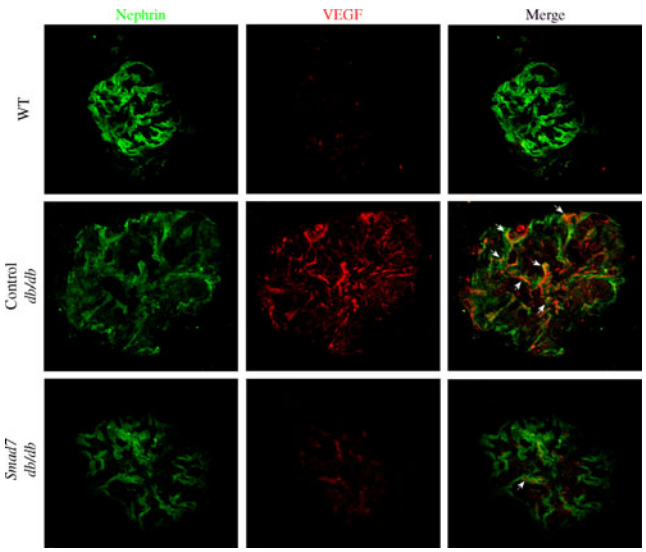

Fig. 3 Podocyte-related protein abundance in the glomerulus from wild-type (WT), control *db*/*db* and *Smad7*-transferred *db*/*db* mice. Immunofluorescence staining of glomeruli with anti-VEGF (red) and anti-nephrin (green) antibodies using confocal laser scanning microscopy. Original magnification ×800. Arrows indicate double positive staining. Images are from a representative experiment on a group of 12 mice

Blocking of TGF-β/SMAD2/3 signalling is a key mechanism by which kidney-targeting Smad7 gene transfer inhibits renal fibrosis and inflammation We next investigated the mechanisms by which SMAD7 inhibited renal fibrosis/sclerosis in the mouse model of type 2 diabetes. As shown in Fig. 5a, b, renal expression of *Tgfb1* mRNA and abundance of TGF-β1 protein were significantly upregulated in control *db*/*db* mice compared with wild-type mice, as demonstrated by real-time PCR and ELISA ($p<0.05$ for both). However, *Smad7*-transferred *db*/*db* mice revealed significantly suppressed expression of *Tgfb1* mRNA and its encoded protein ($p<0.05$ for both). Western blot analysis, moreover, showed greatly enhanced SMAD7 abundance in *Smad7*-transferred *db*/*db* mice compared with wild-type or control *db*/*db* mice ($p<0.01$ for both) (Fig. 5c, d). Although phosphorylation of SMAD3 was significantly enhanced in control *db*/*db* compared with wild-type mice ($p<0.01$) (Fig. 5c, d), this effect was greatly abrogated by the administration of *Smad7* plasmids in *db*/*db* mice ($p<0.01$). We performed immunohistochemistry to confirm the levels of phosphorylated SMAD2/3 protein in renal tissues. *Smad7*-transferred *db*/*db* mice revealed significantly lower numbers of cells with nuclear phosphorylated SMAD2/3 in

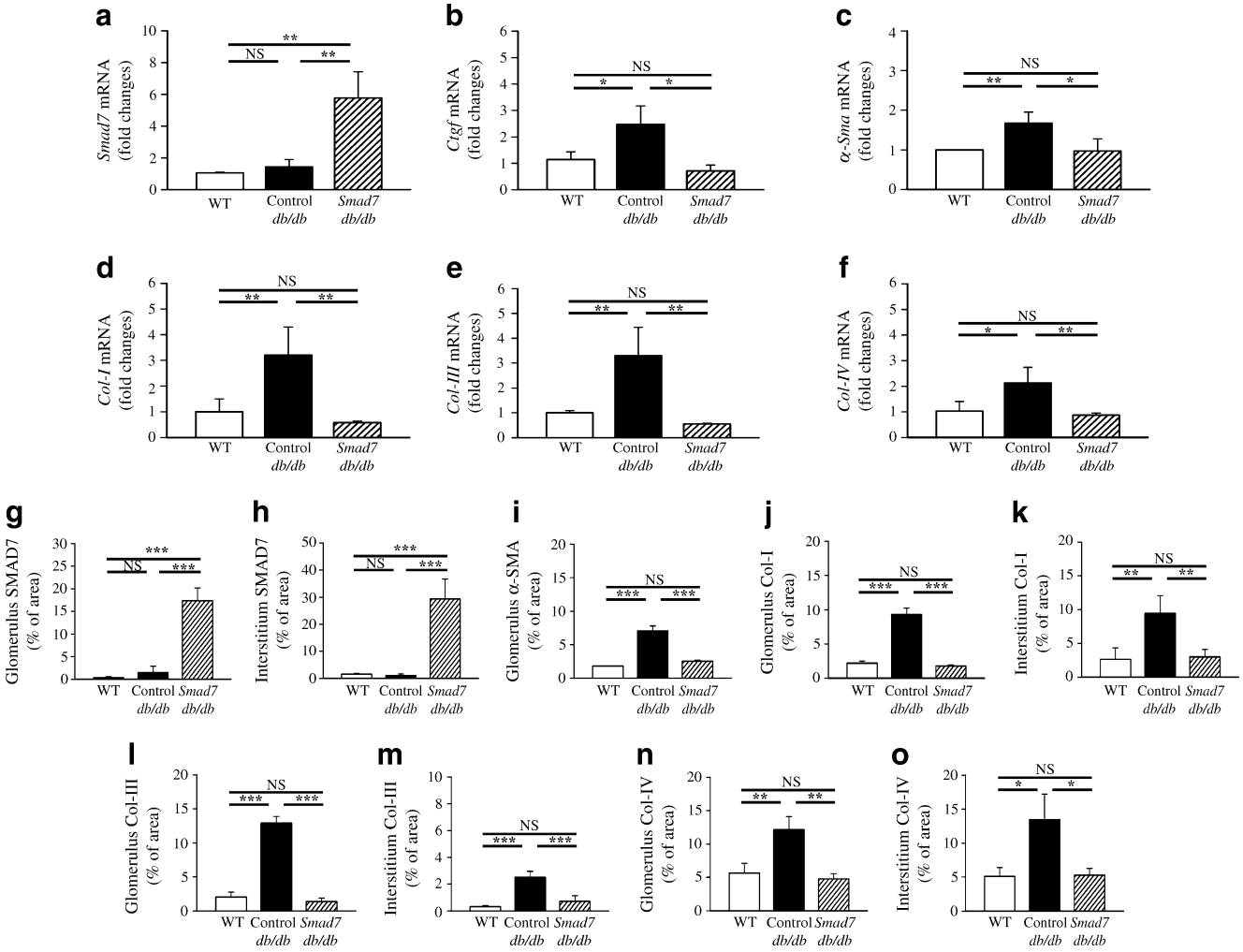

Fig. 4 Renal mRNA expression and protein levels of fibrogenic markers in wild-type (WT, *db/m*), control *db*/*db* and *Smad7*-transferred *db/db* mice. **a** *Smad7*, (**b**) *Ctgf*, (**c**) α-*Sma*, (**d**) *Col-I*, (**e**) *Col-III* and (**f**) *Col-IV* mRNA. **g**, **h** Quantification of SMAD7, (**i**) α-SMA, (**j**, **k**) collagen (Col) I, (**l**, **m**) collagen III and (**n**, **o**) collagen IV protein by immunohistochemistry. Values are the mean ±SEM for a group of 12 mice; *$p<0.05$, **$p<0.01$ and ***$p<0.005$

the kidney than their control counterparts ($p<0.005$) (Fig. 5e, f, ESM Fig. 3). Confocal staining showed that *Smad7*-transferred *db*/*db* mice had less renal nuclear phosphorylated SMAD2/3 in podocytes (Fig. 5g) than control *db*/*db* mice.

It is well established that proinflammatory cytokines can be produced and secreted within the kidney before or after nephritogenic insults [1, 7], and that high blood sugar can cause renal tissue injury and release proinflammatory cytokines in *db*/*db* mice [9, 33]. As shown by real-time PCR, *Smad7*-transferred *db*/*db* mice showed significantly reduced mRNA levels of *Inos* (Fig. 6a), *Il1b* (Fig. 6b) and *Mcp1* (Fig. 6c) in the kidney compared with their control counterparts ($p<0.05$ for each). Immunohistochemical analysis detected significantly lower levels of MCP-1 in the kidney of *Smad7*-transferred *db*/*db* than in control *db*/*db* mice ($p<0.05$) (Fig. 6d, e, ESM Fig. 4a). Moreover, renal macrophages (F4/80) (Fig. 6f, g, ESM Fig. 4b) were significantly inhibited by the transfer of *Smad7* in *db*/*db* mice compared with control. As NF-κB plays a crucial role in initiating inflammation in the kidney with glomerulonephritis, we evaluated the activation of NF-κB in the kidney by immunohistochemistry. Compared with control *db*/*db* mice, the *Smad7*-transferred counterparts showed markedly reduced NF-κB p65 levels in the nuclei of the glomerular cells and renal tubular epithelial cells ($p<0.005$) (Fig. 6h, i, ESM Fig. 4c). This effect was confirmed by ELISA. Although significantly increased nuclear NF-κB p65 protein levels were observed in control *db*/*db* compared with wild-type mice, *Smad7* gene transfer resulted in a substantial reduction of nuclear NF-κB p65 protein in *Smad7*-transferred *db*/*db* mice (Fig. 6j). These findings suggest that kidney-targeting *Smad7* gene transfer resulted in suppressed renal inflammation at least in part via

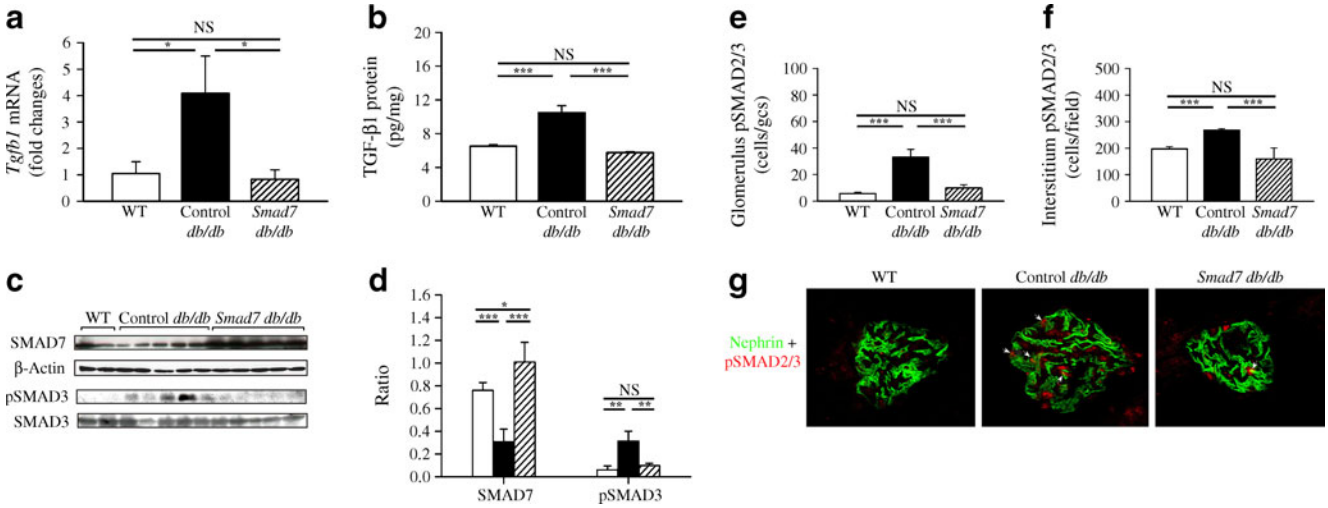

Fig. 5 Renal TGF-β1 abundance and SMAD2/3 activation in wild-type (WT, *db/m*), control *db/db* and *Smad7*-transferred *db/db* mice. **a** *Tgfb1* mRNA in kidney detected by real-time PCR. **b** TGF-β1 protein levels of kidney detected by ELISA. **c** SMAD7 and phosphorylated (p) SMAD3, detected by western blot analysis and (**d**) quantified by semi-quantitative analysis of western blots. White bars, wild-type (*db/m*); black bars, control *db/db*; hatched bars, *Smad7 db/db*. **e**, **f** Quantification of phosphorylated SMAD2/3 nuclear location by immunohistochemistry. gcs, glomerular cross-section. Values (**a**, **b**, **d–f**) are the mean±SEM for a group of 12 mice. *$p<0.05$, **$p<0.01$ and ***$p<0.005$. **g** Immunofluorescence staining of glomerular with anti-phosphorylated SMAD2/3 (red) and anti-nephrin (green) antibodies in tissue as indicated, visualised by confocal laser scanning microscopy. Original magnification ×800. Arrowheads indicate double positive staining

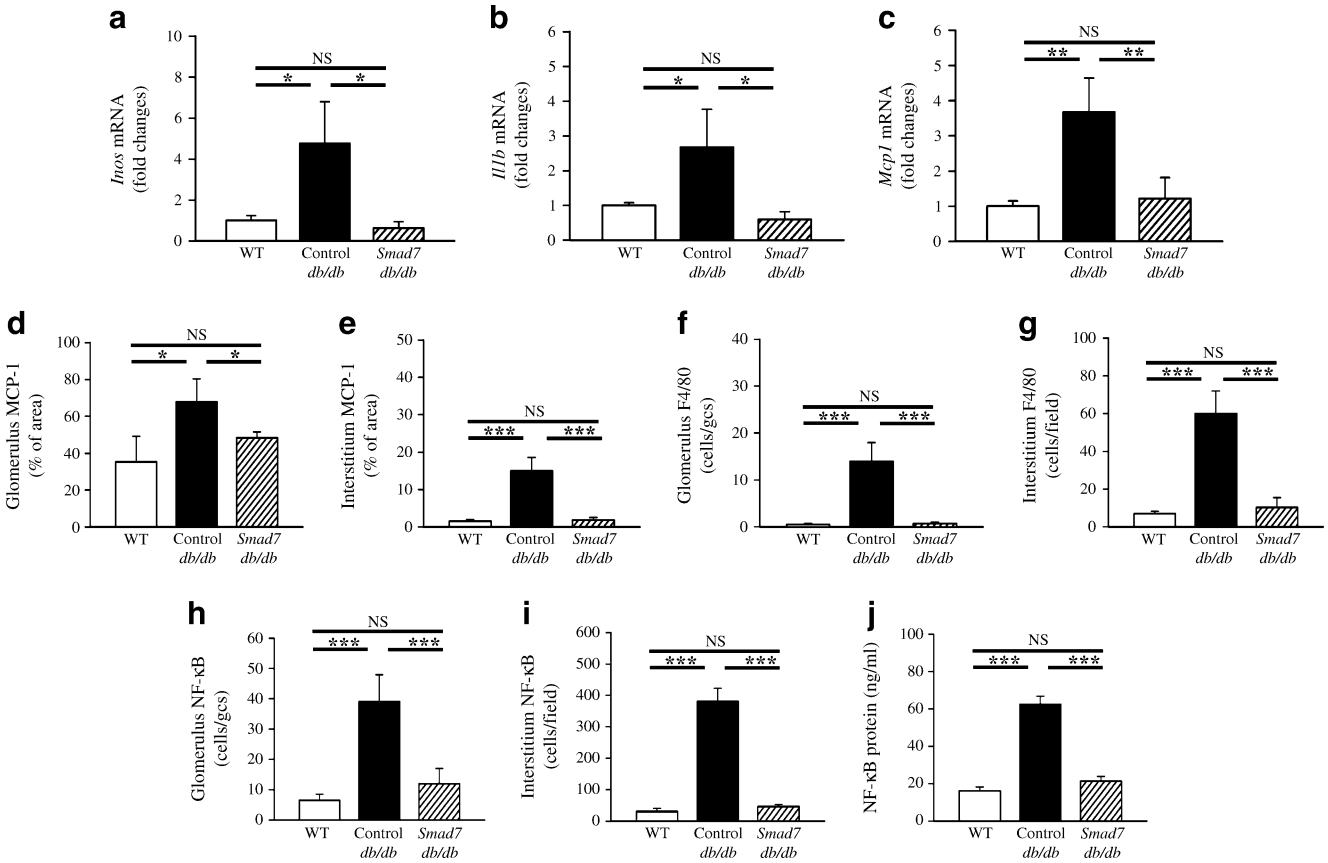

Fig. 6 Renal proinflammatory cytokine expression and abundance in wild-type (WT, *db/m*), control *db/db* and *Smad7*-transferred *db/db* mice. **a** *Inos*, (**b**) *Il1b* and (**c**) *Mcp1* mRNA. Quantification of MCP-1 (**d**, **e**), F4/80 macrophages/monocytes (**f**, **g**) and phosphorylated NF-κB p65 nuclear location (**h**, **i**) by immunohistochemistry in tissue as indicated. **j** Phosphorylated NF-κB p65 activation by ELISA. gcs, glomerular cross-section. Values are the mean±SEM for a group of 12 mice. *$p<0.05$, **$p<0.01$ and ***$p<0.005$

inhibition of renal NF-κB activation in the *Smad7*-transferred animals.

Discussion

Smad7 plasmids were introduced into the kidney of the *db*/*db* mouse model of type 2 diabetes via kidney-targeting, controllable, ultrasound-mediated, microbubble-inducible gene transfer. This caused improvements in: (1) proteinuria and renal function impairment; (2) glomerular mesangial expansion and glomerular sclerosis; (3) focal interstitial mononuclear leucocyte infiltration; and (4) ultrastructural levels of podocyte and endothelial cell injury. These improvements occurred although the severity of hypercholesterolaemia and blood/urine sugar in the *Smad7*-transferred and control *db*/*db* mice was similar at 38 weeks of age. Our data support the concept that organ-targeting *Smad7* gene therapy may have therapeutic effects on the renal fibrosis/sclerosis and inflammatory lesions of diabetic nephropathy, mainly by inducing local production of SMAD7 protein in the kidney, thereby avoiding potential systemic effects from the administration of *Smad7* plasmids.

The anti-inflammatory process resulting from kidney-targeted *Smad7* gene transfer may play an important role in exerting the kidney-protective effect of the procedure [21–23, 26]. We previously demonstrated that overexpression of *Smad7* blocked the renal inflammatory pathway that is dependent on NF-κB activation, thereby inhibiting production of proinflammatory cytokines (e.g. IL-1β, IL-6), adhesion molecules/chemokines (e.g. intercellular adhesion molecule 1, MCP-1) and inducible nitric oxide synthase (iNOS), as well as mononuclear leucocyte infiltration (e.g. $CD4^+$ cells and macrophages) [21]. In the present study, although scattered infiltration of macrophages in the renal interstitium was observed in the *db*/*db* mouse model of type 2 diabetes, this effect was clearly prevented by *Smad7* gene transfer. This suggests that kidney-targeted *Smad7* gene therapy can have potential for the treatment of the renal interstitial inflammation associated with type 2 diabetes. Although it remains unclear whether the advantage resulted from a direct effect, we believe that the route of *Smad7* gene transfer using a kidney-targeting, ultrasound-mediated microbubble system with resultant optimal levels of SMAD7 production locally in the kidney could account for the beneficial effects.

Chen et al. [26] have shown that SMAD7 plays a reno-protective role, while Wang et al. [36] have also demonstrated the effects of *Smad3* knockout as mimicking anti-TGF-β therapy in a model of type 1 diabetes. Here, we have also shown the therapeutic values of kidney-targeting gene therapy for type 2 diabetes, including the favourable effects on podocyte injury and glomerular ultrastructural alterations, suggesting that improvements in intrinsic cells of the glomerulus could be a mechanism driving the SMAD7-mediated reno-protective effects in the development and progression of diabetic nephropathy.

Several glomerular ultrastructural features in the fully developed stage of diabetic nephropathy in the *db*/*db* mouse model of type 2 diabetes have been recognised and have pathogenic implications in the progression of glomerular lesions in type 2 diabetes. These include thickening of the glomerular basement [24, 37] and alterations of podocytes such as increased length of foot processes [37, 38] and multiple focal foot process effacement [25, 39]. We have now added an additional characteristic ultrastructural feature, namely focal but intense villous transformation, detected in *db*/*db* mice by electron microscopy, in addition to focal foot process effacement and projections of the endothelial cell focally in the glomerular tuft area along with microvesicular changes. In the present study, kidney-targeting *Smad7* gene transfer significantly prevented these ultrastructural alterations in endothelial cells and podocytes (Figs 2 and 3) at the dose used throughout the experiment. However, Schiffer et al. [32] demonstrated that SMAD7 is an amplifier of apoptosis in cultured podocytes carrying an adenovirus encoding *Smad7*, and acts through caspase-3- and TGF-β-independent mechanisms. Further investigation to determine the pathogenic pathway in our mouse model of type 2 diabetes is warranted. However, the mechanisms responsible for the favourable effects of *Smad7* gene therapy on glomerular intrinsic cells in the *db*/*db* mouse model of type 2 diabetes remain unclear. It would therefore be worth further dissecting major and direct pathogenic mechanisms, such as pathways involving angiotensin II [40], connective tissue growth factor [41, 42] and prostaglandin E2 [43].

Blockade of the TGF-β-mediated fibrosis pathway via administration of adenoviral dominant TGF-β receptor can suppress mesangial matrix deposition and fibrosis of kidney in a streptozotocin-induced model of type 1 diabetes [2], but this kind of therapeutic module may incur an enhanced inflammatory response, and renal injury has been reported in treatment based on neutralising TGF-β antibodies [8]. In the present study, *Smad7* gene transfer was shown to inhibit mesangial expansion in the glomerulus of *Smad7*-transferred *db*/*db* mice, but no such undesired inflammatory response in the kidney was observed at the dose of *Smad7* plasmids used throughout the experiment.

Wilms tumour 1 (WT-1) has been found to regulate nephrin, suggesting that nephrin acts downstream of WT-1 [44]. It would be worth evaluating WT-1 abundance to determine the colocalisation of nuclear protein and podocyte, although some reports have revealed that nephrin might be a

more representative marker of the glomerular filter than other podocyte molecules [45, 46].

It should be noted that the kidney-targeting *Smad7* transfer alone was not able to completely restore renal function and renal pathology to normal in our study. In addition, we observed no significant effects of the treatment on serum or urinary levels of glucose in *Smad7*-transferred *db*/*db* mice. In this regard, hyperglycaemia has been shown to activate various pathways [47], and evokes mitochondrial dysfunction and renal injury [48]. These effects might account for the incomplete remission of kidney injury in the *Smad7*-transferred *db*/*db* mice, although further investigation on this particular aspect is necessary. Although we demonstrated that blocking of SMAD2/3 activation, NF-κB activation and MCP-1 production in the kidney was associated with the potential mechanisms responsible for the effectiveness of *Smad7* transfer, we did not address by functional studies their relative importance in contributing to the final outcome.

Acknowledgements This study was supported by grants from Tri-Service General Hospital (TSGH-C98-53), Department of Health, Executive Yuan (DOH97-TD-I-11-TM006), and the Ministry of Economic Affairs (99-EC-17-A-19-S1-161), Taiwan, Republic of China.

Contribution statement All authors participated in the conception and design, or analysis and interpretation of the data, contributed to drafting and revising the manuscript, and gave final approval of the version to be published.

Duality of interest The authors declare that there is no duality of interest associated with this manuscript.

References

1. Wolf G, Ritz E (2003) Diabetic nephropathy in type 2 diabetes prevention and patient management. J Am Soc Nephrol 14:1396–1405
2. Kondo T, Takemura G, Kosai K et al (2008) Application of an adenoviral vector encoding soluble transforming growth factor-beta type II receptor to the treatment of diabetic nephropathy in mice. Clin Exp Pharmacol Physiol 35:1288–1293
3. Booth GL, Kapral MK, Fung K, Tu JV (2006) Relation between age and cardiovascular disease in men and women with diabetes compared with non-diabetic people: a population-based retrospective cohort study. Lancet 368:29–36
4. Pagtalunan ME, Miller PL, Jumping-Eagle S et al (1997) Podocyte loss and progressive glomerular injury in type II diabetes. J Clin Invest 99:342–348
5. White KE, Bilous RW (2000) Type 2 diabetic patients with nephropathy show structural–functional relationships that are similar to type 1 disease. J Am Soc Nephrol 11:1667–1673
6. Mason RM, Wahab NA (2003) Extracellular matrix metabolism in diabetic nephropathy. J Am Soc Nephrol 14:1358–1373
7. Chow F, Ozols E, Nikolic-Paterson DJ, Atkins RC, Tesch GH (2004) Macrophages in mouse type 2 diabetic nephropathy: correlation with diabetic state and progressive renal injury. Kidney Int 65:116–128
8. Ziyadeh FN, Hoffman BB, Han DC et al (2000) Long-term prevention of renal insufficiency, excess matrix gene expression, and glomerular mesangial matrix expansion by treatment with monoclonal antitransforming growth factor-beta antibody in *db*/*db* diabetic mice. Proc Natl Acad Sci USA 97:8015–8020
9. Stolar M (2010) Glycemic control and complications in type 2 diabetes mellitus. Am J Med 123:S3–S11
10. Petersen M, Thorikay M, Deckers M et al (2008) Oral administration of GW788388, an inhibitor of TGF-b type I and II receptor kinases, decreases renal fibrosis. Kidney Int 73:705–715
11. Jiang T, Huang Z, Lin Y, Zhang Z, Fang D, Zhang DD (2010) The protective role of Nrf2 in streptozotocin-induced diabetic nephropathy. Diabetes 59:850–860
12. Kikkawa R, Umemura K, Haneda M, Arimura T, Ebata K, Shigeta Y (1987) Evidence for existence of polyol pathway in cultured rat mesangial cells. Diabetes 36:240–243
13. Yokoyama H, Deckert T (1996) Central role of TGF-beta in the pathogenesis of diabetic nephropathy and macrovascular complications: a hypothesis. Diabet Med 13:313–320
14. Yamamoto T, Noble NA, Cohen AH et al (1996) Expression of transforming growth factor-beta isoforms in human glomerular diseases. Kidney Int 49:461–469
15. Gupta S, Clarkson MR, Duggan J, Brady HR (2000) Connective tissue growth factor: potential role in glomerulosclerosis and tubulointerstitial fibrosis. Kidney Int 58:1389–1399
16. Ma LJ, Jha S, Ling H, Pozzi A, Ledbetter S, Fogo AB (2004) Divergent effects of low versus high dose anti-TGF-beta antibody in puromycin aminonucleoside nephropathy in rats. Kidney Int 65:106–115
17. Hayashi H, Abdollah S, Qiu Y et al (1997) The MAD-related protein Smad7 associates with the TGFbeta receptor and functions as an antagonist of TGFbeta signaling. Cell 89:1165–1173
18. Kavsak P, Rasmussen RK, Causing CG et al (2000) Smad7 binds to Smurf2 to form an E3 ubiquitin ligase that targets the TGF beta receptor for degradation. Mol Cell 6:1365–1375
19. Ng YY, Hou CC, Wang W, Huang XR, Lan HY (2005) Blockade of NFkappaB activation and renal inflammation by ultrasound-mediated gene transfer of Smad7 in rat remnant kidney. Kidney Int Suppl S83–S91
20. Wang W, Huang XR, Li AG et al (2005) Signaling mechanism of TGF-beta1 in prevention of renal inflammation: role of Smad7. J Am Soc Nephrol 16:1371–1383
21. Ka SM, Huang XR, Lan HY et al (2007) Smad7 gene therapy ameliorates an autoimmune crescentic glomerulonephritis in mice. J Am Soc Nephrol 18:1777–1788
22. Lan HY, Mu W, Tomita N et al (2003) Inhibition of renal fibrosis by gene transfer of inducible Smad7 using ultrasound-microbubble system in rat UUO model. J Am Soc Nephrol 14:1535–1548
23. Hou CC, Wang W, Huang XR et al (2005) Ultrasound-microbubble-mediated gene transfer of inducible Smad7 blocks transforming growth factor-beta signaling and fibrosis in rat remnant kidney. Am J Pathol 166:761–771
24. Sharma K, McCue P, Dunn SR (2003) Diabetic kidney disease in the *db*/*db* mouse. Am J Physiol Renal Physiol 284:F1138–F1144
25. Huang Y, Border WA, Yu L, Zhang J, Lawrence DA, Noble NA (2008) A PAI-1 mutant, PAI-1R, slows progression of diabetic nephropathy. J Am Soc Nephrol 19:329–338
26. Chen HY, Huang XR, Wang W et al (2011) The protective role of Smad7 in diabetic kidney disease: mechanism and therapeutic potential. Diabetes 60:590–601
27. Summy-Long JY, Hu S (2009) Peripheral osmotic stimulation inhibits the brain's innate immune response to microdialysis of acidic perfusion fluid adjacent to supraoptic nucleus. Am J Physiol Regul Integr Comp Physiol 297:R1532–R1545

28. de Vriese AS, Tilton RG, Elger M, Stephan CC, Kriz W, Lameire NH (2001) Antibodies against vascular endothelial growth factor improve early renal dysfunction in experimental diabetes. J Am Soc Nephrol 12:993–1000
29. Flyvbjerg A, Dagnaes-Hansen F, de Vriese AS, Schrijvers BF, Tilton RG, Rasch R (2002) Amelioration of long-term renal changes in obese type 2 diabetic mice by a neutralizing vascular endothelial growth factor antibody. Diabetes 51:3090–3094
30. Ka SM, Sytwu HK, Chang DM, Hsieh SL, Tsai PY, Chen A (2007) Decoy receptor 3 ameliorates an autoimmune crescentic glomerulonephritis model in mice. J Am Soc Nephrol 18:2473–2485
31. Cheng CW, Rifai A, Ka SM et al (2005) Calcium-binding proteins annexin A2 and S100A6 are sensors of tubular injury and recovery in acute renal failure. Kidney Int 68:2694–2703
32. Schiffer M, Bitzer M, Roberts IS et al (2001) Apoptosis in podocytes induced by TGF-β and Smad7. J Clin Invest 108:807–816
33. Susztak K, Raff AC, Schiffer M, Böttinger EP (2006) Glucose-induced reactive oxygen species cause apoptosis of podocytes and podocyte depletion at the onset of diabetic nephropathy. Diabetes 55:225–233
34. Mishra R, Emancipator SN, Kern T, Simonson MS (2005) High glucose evokes an intrinsic proapoptotic signaling pathway in mesangial cells. Kidney Int 67:82–93
35. Brezniceanu ML, Liu F, Wei CC et al (2008) Attenuation of interstitial fibrosis and tubular apoptosis in *db*/*db* transgenic mice overexpressing catalase in renal proximal tubular cells. Diabetes 57:451–459
36. Wang A, Ziyadeh FN, Lee EY et al (2007) Interference with TGF-beta signaling by Smad3-knockout in mice limits diabetic glomerulosclerosis without affecting albuminuria. Am J Physiol Renal Physiol 293:F1657–F1665
37. Zhao HJ, Wang S, Cheng H et al (2006) Endothelial nitric oxide synthase deficiency produces accelerated nephropathy in diabetic mice. J Am Soc Nephrol 17:2664–2669
38. Wang Z, Jiang T, Li J et al (2005) Regulation of renal lipid metabolism, lipid accumulation, and glomerulosclerosis in FVB *db*/*db* mice with type 2 diabetes. Diabetes 54:2328–2335
39. Hong SW, Isono M, Chen S, Iglesias-De La Cruz MC, Han DC, Ziyadeh FN (2001) Increased glomerular and tubular expression of transforming growth factor-beta1, its type II receptor, and activation of the Smad signaling pathway in the *db*/*db* mouse. Am J Pathol 158:1653–1663
40. Whaley-Connell A, Habibi J, Nistala R et al (2008) Attenuation of NADPH oxidase activation and glomerular filtration barrier remodeling with statin treatment. Hypertension 51:474–480
41. Lee HS (2011) Pathogenic role of TGF-β in the progression of podocyte diseases. Histol Histopathol 26:107–116
42. Ito Y, Goldschmeding R, Kasuga H et al (2010) Expression patterns of connective tissue growth factor and of TGF-beta isoforms during glomerular injury recapitulate glomerulogenesis. Am J Physiol Renal Physiol 299:F545–F558
43. Faour WH, Thibodeau JF, Kennedy CR (2010) Mechanical stretch and prostaglandin E2 modulate critical signaling pathways in mouse podocytes. Cell Signal 22:1222–1230
44. Guo JK, Menke AL, Gubler MC et al (2002) WT1 is a key regulator of podocyte function: reduced expression levels cause crescentic glomerulonephritis and mesangial sclerosis. Hum Mol Genet 11:651–659
45. Fan Q, Xing Y, Ding J, Guan N, Zhang J (2006) The relationship among nephrin, podocin, CD2AP, and alpha-actinin might not be a true 'interaction' in podocyte. Kidney Int 69:1207–1215
46. Yuan H, Takeuchi E, Taylor GA, McLaughlin M, Brown D, Salant DJ (2002) Nephrin dissociates from actin, and its expression is reduced in early experimental membranous nephropathy. J Am Soc Nephrol 13:946–956
47. Choudhury D, Tuncel M, Levi M (2010) Diabetic nephropathy—a multifaceted target of new therapies. Discov Med 10:406–415
48. Vanhorebeek I, Gunst J, Ellger B et al (2009) Hyperglycemic kidney damage in an animal model of prolonged critical illness. Kidney Int 76:512–520